Ann. Scient. Éc. Norm. Sup.
4ᵉ série, t. 52, 2019, p. 367 à 392

ACYLINDRICAL HYPERBOLICITY OF THE THREE-DIMENSIONAL TAME AUTOMORPHISM GROUP

BY STÉPHANE LAMY AND PIOTR PRZYTYCKI

ABSTRACT. – We prove that the group STame($\mathbf{k}^3$) of special tame automorphisms of the affine 3-space is not simple, over any base field of characteristic zero. Our proof is based on the study of the geometry of a 2-dimensional simply-connected simplicial complex $\mathcal{C}$ on which the tame automorphism group acts naturally. We prove that $\mathcal{C}$ is contractible and Gromov-hyperbolic, and we prove that Tame($\mathbf{k}^3$) is acylindrically hyperbolic by finding explicit loxodromic weakly proper discontinuous elements.

RÉSUMÉ. – Nous montrons que le groupe STame($\mathbf{k}^3$) des automorphismes modérés unimodulaires de l'espace affine de dimension 3 n'est pas simple, sur tout corps de base de caractéristique zéro. Notre preuve repose sur l'étude géométrique d'un complexe simplicial $\mathcal{C}$ simplement connexe et de dimension 2, sur lequel le groupe des automorphismes modérés agit naturellement. Nous montrons que $\mathcal{C}$ est contractible et hyperbolique au sens de Gromov, puis nous prouvons que Tame($\mathbf{k}^3$) est acylindriquement hyperbolique en exhibant des éléments loxodromiques satisfaisant la propriété WPD.

1. Introduction

The *tame automorphism group* of the affine space $\mathbf{k}^3$, over a base field $\mathbf{k}$ of characteristic zero, is the subgroup of the polynomial automorphism group $\mathrm{Aut}(\mathbf{k}^3)$ generated by the affine and elementary automorphisms:

$$\mathrm{Tame}(\mathbf{k}^3) = \langle A_3, E_3 \rangle,$$

where

$$A_3 = \mathrm{GL}_3(\mathbf{k}) \ltimes \mathbf{k}^3, \text{ and}$$
$$E_3 = \{(x_1, x_2, x_3) \mapsto (x_1 + P(x_2, x_3), x_2, x_3) \mid P \in \mathbf{k}[x_2, x_3]\}.$$

The first author's research was partially supported by ANR Grant "BirPol" ANR-11-JS01-004-01. The second author was partially supported by NSERC, FRQNT, National Science Centre DEC-2012/06/A/ST1/00259, and UMO-2015/18/M/ST1/00050.

doi:10.24033/asens.2390

There is a natural homomorphism Jac: $\mathrm{Tame}(\mathbf{k}^3) \to \mathbf{k}^*$ given by the Jacobian determinant. The kernel $\mathrm{STame}(\mathbf{k}^3)$ of this homomorphism is the *special tame automorphism group*. Analogously one defines $\mathrm{Tame}(\mathbf{k}^n)$ and $\mathrm{STame}(\mathbf{k}^n)$ for arbitrary $n \geqslant 2$. It is a natural question whether $\mathrm{STame}(\mathbf{k}^n)$ is a simple group. In this paper we prove that $\mathrm{STame}(\mathbf{k}^3)$ is not simple (and indeed very far from being simple).

Our strategy is to use an action of $\mathrm{Tame}(\mathbf{k}^3)$ on a Gromov-hyperbolic triangle complex, and to exhibit a loxodromic weakly proper discontinuous element of $\mathrm{STame}(\mathbf{k}^3)$, in the sense of M. Bestvina and K. Fujiwara [1]. Recall that an isometry f of a metric space X is *loxodromic* if for some (hence any) $x \in X$ there exists $\lambda > 0$ such that for any $k \in \mathbb{Z}$ we have $|x, f^k \cdot x| \geqslant \lambda |k|$. Suppose that f belongs to a group G acting on X by isometries. We say that f is *weakly proper discontinuous* (WPD) if for some (hence any) $x \in X$ and any $C \geqslant 1$, for k sufficiently large there are only finitely many $j \in G$ satisfying $|x, j \cdot x| \leqslant C$ and $|f^k \cdot x, j \circ f^k \cdot x| \leqslant C$.

By the work of F. Dahmani, V. Guirardel, and D. Osin [8, Thm 8.7], the existence of an action of a non-virtually cyclic group G on a Gromov-hyperbolic metric space, with at least one loxodromic WPD element, implies that G has a free normal subgroup, and in particular G is not simple. By the work of D. Osin [18, Thm 1.2], such a group is *acylindrically hyperbolic*: there exists a (different) Gromov-hyperbolic space on which the action of G is acylindrical, a notion introduced for general metric spaces by B. Bowditch [3].

This strategy was recently applied to various transformation groups in algebraic geometry. We now review a few examples to explain how the group $\mathrm{Tame}(\mathbf{k}^3)$ fits in the global picture.

First we discuss the group $\mathrm{Bir}(\mathbb{P}^2_{\mathbf{k}})$, the *Cremona group* of rank 2, which is the group of birational transformations of the projective plane. It is by no means obvious to find a Gromov-hyperbolic space on which the Cremona groups acts. One takes all projective surfaces dominating $\mathbb{P}^2_{\mathbf{k}}$ by a sequence of blow-ups, and considers the direct limit of their spaces of curves, called Néron-Severi groups. The limit is endowed with a lorentzian intersection form defining an infinite dimensional hyperboloid. This hyperboloid was introduced in [5] and used to prove for instance a Tits alternative for the Cremona group. Then it was used in [7] to prove the non-simplicity of $\mathrm{Bir}(\mathbb{P}^2_{\mathbf{k}})$ over an algebraically closed field $\mathbf{k}$. Finally, the above mentioned strategy was applied in [14] to obtain the non-simplicity over an arbitrary base field.

Note that one of the initial motivations for [8] was the application to the mapping class group. As it is the case for the Cremona group, in studying the mapping class group one uses an action on a non-locally compact Gromov-hyperbolic space (the complex of curves), but the parallel goes beyond that. For instance, there are striking similarities between the notion of dilatation factor for a pseudo-Anosov map, and the dynamical degree of a generic Cremona map: see the survey [6] for more details.

The above results about $\mathrm{Bir}(\mathbb{P}^2_{\mathbf{k}})$ were inspired by previous work on its subgroup $\mathrm{Aut}(\mathbf{k}^2) = \mathrm{Tame}(\mathbf{k}^2)$. It is classical that $\mathrm{Aut}(\mathbf{k}^2)$ is the amalgamated product of two of its subgroups, and so we get an action of $\mathrm{Aut}(\mathbf{k}^2)$ on the associated Bass-Serre tree (which is obviously Gromov-hyperbolic). Together with some classical small cancelation theory this was used by V. Danilov [9] to produce many normal subgroups in $\mathrm{Aut}(\mathbb{C}^2)$ (and in $\mathrm{SAut}(\mathbb{C}^2)$), see also [10]. Recently these results were extended to the case of an arbitrary

field by A. Minasyan and D. Osin [17, Cor 2.7], again by producing concrete examples of WPD elements.

When one tries to extend these results to higher dimensions, one has to face the formidable gap in complexity between birational geometry of surfaces and in higher dimension. We refer to the introduction of [2] for a few more comments on this side of the story. The group Tame($\mathbf{k}^3$) seems to be a good first step to enter the world of dimension 3. It was a classical question proposed by M. Nagata in the 70' whether the inclusion Tame($\mathbf{k}^3$) $\subset$ Aut($\mathbf{k}^3$) was strict. This was confirmed 30 years later by I.P. Shestakov and U.U. Umirbaev [20], with an argument which was somewhat simplified by S. Kuroda [12]. Then it was recently noticed [2, 21, 13] that we can rephrase the theory developped by these authors by saying that Tame($\mathbf{k}^3$) is the amalgamated product of three subgroups along their pairwise intersections. Equivalently, the group Tame($\mathbf{k}^3$) acts on a simply connected 2-dimensional simplicial complex $\mathcal{C}$, with fundamental domain a single triangle. This complex $\mathcal{C}$ is the main object of our present work (see Section 2 for the definition).

To end the historical background, note that the situation on the affine 3-dimensional quadric has been also successfully explored. (In fact, we considered it a test setting for the whole strategy, before trying to handle the affine space $\mathbf{k}^3$.) The notion of a tame automorphism in this context was introduced by S. Vénéreau and the first author. An action on a Gromov-hyperbolic CAT(0) square complex was constructed in [2]. WPD elements were recently produced by A. Martin [16].

Our first two results about the geometry of the complex $\mathcal{C}$ associated with Tame($\mathbf{k}^3$) are the following.

THEOREM A. – *$\mathcal{C}$ is contractible.*

THEOREM B. – *$\mathcal{C}$ is Gromov-hyperbolic.*

As is often the case when dealing with 2-dimensional complexes, our arguments rely on understanding disk diagrams, i.e., simplicial disks mapping to the complex. The main difficulty here is that, by contrast with the above mentioned settings, the complex $\mathcal{C}$ does not admit an equivariant CAT(0) metric. We circumvent this problem by a procedure of "transport of curvature". Precisely, given a disk diagram, first we assign to each triangle of the diagram angles $\pi/2, \pi/3, \pi/6$, and then, by putting an orientation on certain edges of the diagram, we describe how to transport any excess of positive curvature at a given vertex to neighboring vertices. In this sense we obtain that any disk diagram is negatively curved, which gives Theorem A, and also, via linear isoperimetric inequality, Theorem B.

We now turn to the existence of WPD elements in Tame($\mathbf{k}^3$). On the 1-skeleton $\mathcal{C}^1$ of $\mathcal{C}$ we use the path metric where each edge has length 1, which is quasi-isometric to any Tame($\mathbf{k}^3$)-equivariant path-metric on $\mathcal{C}$. Let $n \geqslant 0$, and let $g, h, f \in$ Tame($\mathbf{k}^3$) be the automorphisms defined by

$$\begin{aligned} g^{-1}(x_1, x_2, x_3) &= (x_2, x_1 + x_2 x_3, x_3), \\ h^{-1}(x_1, x_2, x_3) &= (x_3, x_1, x_2), \\ f &= g^n \circ h. \end{aligned}$$

Observe that $\mathrm{Jac}(h) = 1$ and $\mathrm{Jac}(g) = -1$, so for even n the automorphism f is an element of $\mathrm{STame}(\mathbf{k}^3)$.

THEOREM C. – *Let $n \geqslant 3$. Then f acts as a loxodromic element on $\mathcal{C}^1$. In particular, the complex $\mathcal{C}$ has infinite diameter.*

THEOREM D. – *Let $n \geqslant 12$ be even and $G = \mathrm{Tame}(\mathbf{k}^3)$. Then f acts as a* WPD *element on $\mathcal{C}^1$.*

Again the idea of proof relies on the notion of combinatorial curvature. There is a simplicial embedding $\gamma\colon \mathbb{R} \to \mathcal{C}$ such that f acts by translation on the image of γ. Moreover, we prove that any disk diagram containing a segment of γ in its boundary has very negative curvature along this segment. This is the key property that allows to obtain both Theorems C and D.

As mentioned above, by [8, Thm 8.7], Theorems C and D immediately imply the following:

COROLLARY E. – *The group $\mathrm{STame}(\mathbf{k}^3)$ is not simple.*

Furthermore, by [18, Thm 1.2], we have:

COROLLARY F. – *The groups $\mathrm{Tame}(\mathbf{k}^3)$ and $\mathrm{STame}(\mathbf{k}^3)$ are acylindrically hyperbolic.*

Organization. – We recall the definition of $\mathcal{C}$ in Section 2. In Section 3 we study its local geometry. This allows us in Section 4 to introduce the *curvature* at vertices of reduced disk diagrams in $\mathcal{C}$. In Section 5 we prove that curvature is nonpositive and we deduce Theorem A. A more detailed study allows to prove Theorem B in Section 6. Finally, in Section 7 we prove Theorems C and D.

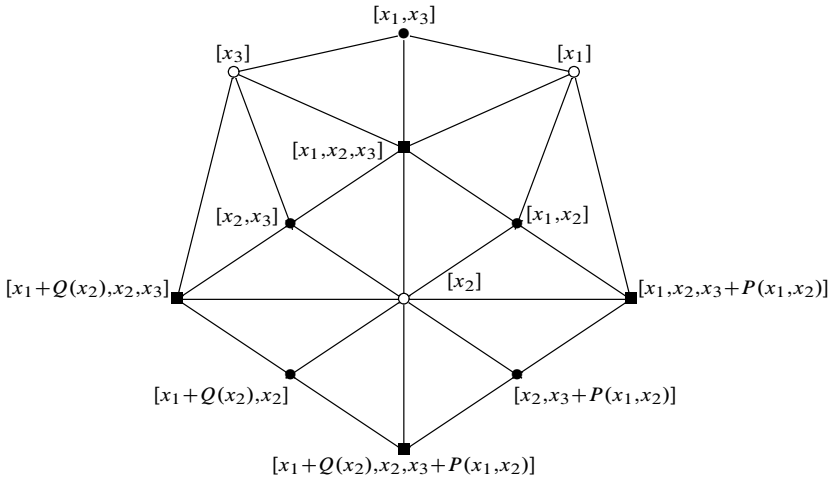

FIGURE 1. Some triangles of the complex $\mathcal{C}$

2. Complex

In this section we recall the construction of the simplicial complex $\mathcal{C}_n$ associated with Tame($\mathbf{k}^n$), for $n \geqslant 2$. See [2, §2.5], [13] for more details. For any $1 \leqslant r \leqslant n$, an *r-tuple of components* is a polynomial map

$$f : \mathbf{k}^n \to \mathbf{k}^r$$
$$x = (x_1, \ldots, x_n) \mapsto (f_1(x), \ldots, f_r(x))$$

that can be extended to a tame automorphism $f = (f_1, \ldots, f_n)$ of $\mathbf{k}^n$. We consider the orbits of the action of the affine automorphism group $A_r = \mathrm{GL}_r(\mathbf{k}) \ltimes \mathbf{k}^r$ on the r-tuples of components:

$$[f_1, \ldots, f_r] = A_r(f_1, \ldots, f_r) = \{a \circ (f_1, \ldots, f_r) \mid a \in A_r\}.$$

A *vertex of type r* of $\mathcal{C}_n$ is such an orbit $[f_1, \ldots, f_r]$, and will be usually denoted as v_r. The vertices $[f_1], [f_1, f_2], \ldots, [f_1, \ldots, f_n]$ span an $(n-1)$-simplex of $\mathcal{C}_n$. The tame automorphism group acts on $\mathcal{C}_n$ by isometries, via pre-composition:

$$g \cdot [f_1, \ldots, f_r] = [f_1 \circ g^{-1}, \ldots, f_r \circ g^{-1}].$$

Note that this action is transitive on $(n-1)$-simplices, and in particular, it is transitive on the vertices of any type. It is easy to see that $\mathcal{C}_n$ is connected.

We shall use $\mathcal{C}_n$ mainly in the case $n = 3$, but also in the case $n = 2$, to study the link of a vertex in $\mathcal{C}_3$. In fact, $\mathcal{C}_2$ is the Bass-Serre tree corresponding to the splitting $\mathrm{Aut}(\mathbf{k}^2) = A_2 *_{A_2 \cap E_2} E_2$, with

$$E_2 = \{(x_1, x_2) \mapsto (ax_1 + P(x_2), bx_2 + c) \mid a, b \in \mathbf{k}^*, c \in \mathbf{k}, P \in \mathbf{k}[x_2]\}$$

(see [2, Prop 2.16]). We will also denote $\mathcal{C}_2$ as $\mathscr{T}_{\mathbf{k}}$ to emphasize the field. Later also the field $\mathbf{k}(x_3)$ will be used instead of $\mathbf{k}$. We shortly denote by $\mathcal{C} = \mathcal{C}_3$ the triangle complex for Tame($\mathbf{k}^3$). It has vertices of type 1, 2 and 3. We say that an edge in $\mathcal{C}$ has *type* (i, j) if it joins a vertex of type i with a vertex of type j. By $\mathcal{C}^0$, $\mathcal{C}^1$ we denote the vertex set and the 1-skeleton of $\mathcal{C}$.

We illustrate a part of $\mathcal{C}$ in Figure 1. Vertices of types 1, 2, and 3 are represented by symbols $\circ$, $\bullet$, $\blacksquare$, respectively.

3. Trees and links

In this section we define and explain the relation between four trees related to the complex $\mathcal{C}$. The first is the tree $\mathscr{T}_{\mathbf{k}} = \mathcal{C}_2$ with the action of $\mathrm{Aut}(\mathbf{k}^2)$. We will define a second tree $\mathscr{T}(v_2) \subset \mathcal{C}$ associated with each type 2 vertex v_2, isomorphic to $\mathscr{T}_{\mathbf{k}}$. Thirdly, we have the tree $\mathscr{T}_{\mathbf{k}(x)}$ (which is the complex $\mathcal{C}_2$ constructed starting from the field $\mathbf{k}(x)$ instead of $\mathbf{k}$). Finally, we will have a tree $\mathscr{T}(v_1)$ associated to each type 1 vertex v_1, appearing in a sequence of simplicial projections $\mathscr{L}(v_1) \to \mathscr{T}(v_1) \to \mathscr{T}_{\mathbf{k}(x)}$, where $\mathscr{L}(v_1)$ is the link of v_1.

3.1. Tree associated with a type 2 vertex

For any vertex v_2 of $\mathcal{C}$ of type 2 we define the following tree $\mathscr{T}(v_2) \subset \mathcal{C}^1$. We require the definition to be Tame($\mathbf{k}^3$)-equivariant, and hence by the transitivity of the action we can assume that $v_2 = [x_1, x_2]$. Then we consider all vertices of the form $[f_1(x_1, x_2)]$ and $[f_1(x_1, x_2), f_2(x_1, x_2)]$, where $(f_1, f_2) \in \mathrm{Tame}(\mathbf{k}^2)$. These vertices span a tree $\mathscr{T}(v_2)$ isomorphic to $\mathscr{T}_{\mathbf{k}}$. Observe that the embedding $\mathscr{T}(v_2) \subset \mathcal{C}$ is not an isometric embedding, since $\mathscr{T}(v_2)$ is contained in the link of a type 1 vertex v_1 (for example, if $v_2 = [x_1, x_2]$, then one can take $v_1 = [x_3]$).

We now prove a preparatory lemma about leading terms in the vertices of the tree $\mathscr{T}_{\mathbf{k}}$.

LEMMA 3.1. – *Let $[f]$ be a type 1 vertex in $\mathscr{T}_{\mathbf{k}}$, and consider the connected components of the tree $\mathscr{T}_{\mathbf{k}}$ with the vertex $[x_1, x_2]$ removed.*

1. *For the unique $(a : b) \in \mathbb{P}^1_{\mathbf{k}}$ such that $[f]$ and $[ax_1 + bx_2]$ belong to the same component, we have*
$$f(x_1, x_2) = c(ax_1 + bx_2)^d + R(x_1, x_2),$$
with $c \in \mathbf{k}^*$, $d \geqslant 1$, and $\deg R < d$.
2. *Assume that $[f] \neq [x_2]$ belong to the same component. Then*
$$f(x_1, x_2) = Q(x_2)x_2^{d+1} + cx_1x_2^d + R(x_1, x_2),$$
with $c \in \mathbf{k}^*$, $d \geqslant 0$, $\deg R < d + 1$, and Q nonconstant.

   In particular, if $A \in \mathbf{k}[X]$ is any nonconstant polynomial, then $A(f(x_1, x_2))$ has the same form.

Proof. – By definition, vertices in the link of $[x_1, x_2]$ are of the form $[ax_1 + bx_2]$. Moreover, since the stabilizer of $[x_1, x_2]$ is isomorphic to $A_2 = \mathrm{GL}_2(\mathbf{k}) \rtimes \mathbf{k}^2$, it acts transitively on these vertices. So it is sufficient to consider the case where $[f]$ belongs to the same component as $[x_2]$, and to prove assertion (2). In fact we are going to prove that the consecutive type 1 vertices $[f_0] = [x_2], \ldots, [f_n] = [f]$ in the unique embedded path from $[x_2]$ to $[f]$ are of the form (for $i = 1, \ldots, n$)

$$(\star) \qquad f_i(x_1, x_2) = Q_i(x_2)x_2^{d_i+1} + c_ix_1x_2^{d_i} + \text{lower order terms},$$

with the exponents d_i strictly increasing with i, and Q_i nonconstant.

Observe that from Section 2 it follows that for vertices $[g_1], [g_3]$ in $\mathscr{T}_{\mathbf{k}}$ joined by an embedded path of length four with center $[g_2]$, the vertex $[g_3]$ has the form $[g_1 + P(g_2)]$, for some polynomial $P(X)$ that is non-affine, i.e., not of the form $aX + b$.

Applying this observation to $g_1 = x_1, g_2 = x_2, g_3 = f_1$, we obtain $(\star)$ for $i = 1$, with $d_1 = 0$. Then we proceed by induction and assume that for some $j \geqslant 2$, we proved $(\star)$ for all $i < j$. Then applying the observation above to $g_1 = f_{j-2}, g_2 = f_{j-1}, g_3 = f_j$, we arrive at $(\star)$ for $i = j$, with $d_j > d_{j-1}$. □

3.2. Links

It is an easy observation (see [13, §1.C]) that the link $\mathcal{L}(v_2)$ of a vertex of type 2 in the complex $\mathcal{C}$ is a full bipartite graph, and the link $\mathcal{L}(v_3)$ of a vertex of type 3 is the incidence graph of the projective plane $\mathbb{P}^2_{\mathbf{k}}$. Now we study the link $\mathcal{L}(v_1)$ of a vertex of type 1 in $\mathcal{C}$. We know from [13, Lem 5.6] that $\mathcal{L}(v_1)$ is connected. By transitivity of the action we can assume that $v_1 = [x_3]$. We describe two trees related to $\mathcal{L}([x_3])$.

Let π be the simplicial map from $\mathcal{L}([x_3])$ to the tree $\mathcal{T}_{\mathbf{k}(x_3)}$ (see Section 2) mapping $[f_1, x_3]$ to $[f_1]$ and $[f_1, f_2, x_3]$ to $[f_1, f_2]$. The map π is $\mathrm{Stab}([x_3])$-equivariant. Since $\mathcal{L}([x_3])$ is connected, the image $\pi(\mathcal{L}([x_3]))$ is a subtree of $\mathcal{T}_{\mathbf{k}(x_3)}$. The group $\mathrm{Stab}([x_3])$ acts transitively on the edges of $\mathcal{L}([x_3])$, hence transitively on the edges of $\pi(\mathcal{L}([x_3]))$. Denote by $H_1 \subset \mathrm{Stab}([x_3])$ the stabilizer of $\pi^{-1}([x_1])$ and by $H_2 \subset \mathrm{Stab}([x_3])$ the stabilizer of $\pi^{-1}([x_1, x_2])$. By Bass-Serre theory we obtain:

LEMMA 3.2. – *We have*

$$\mathrm{Stab}([x_3]) = H_1 *_{H_1 \cap H_2} H_2.$$

We can give explicit descriptions of H_1 and H_2 (compare with [2, §4.1]).

LEMMA 3.3. – *We have*

$$\begin{aligned}
H_1 &= \{(ax_1 + t(x_3),\ dx_2 + P(x_1, x_3),\ \alpha x_3 + \beta) \mid a, d \in \mathbf{k}^*\},\\
H_2 &= \left\{\left(a(x_3)x_1 + b(x_3)x_2 + t(x_3),\ c(x_3)x_1 + d(x_3)x_2 + t'(x_3),\ \alpha x_3 + \beta\right)\right\}\\
&\simeq \left(\mathrm{GL}_2(\mathbf{k}[x_3]) \ltimes \mathbf{k}[x_3]^2\right) \rtimes A_1,\\
H_1 \cap H_2 &= \left\{\left(ax_1 + t(x_3),\ dx_2 + c(x_3)x_1 + t'(x_3),\ \alpha x_3 + \beta\right) \mid a, d \in \mathbf{k}^*\right\}.
\end{aligned}$$

Proof. – Take $[f_1, x_3] \in \pi^{-1}([x_1])$, that is, $[f_1] = [x_1]$ in the tree $\mathcal{T}_{\mathbf{k}(x_3)}$.

So $f_1 = a(x_3)x_1 + t(x_3)$ for some polynomials a, t, and moreover by definition there exists $f_2 \in \mathbf{k}[x_1, x_2, x_3]$ such that $f = (f_1, f_2, x_3) \in \mathrm{Tame}(\mathbf{k}^3)$. In particular the Jacobian of f is a multiple of a, so a must be a constant. We obtain

$$\pi^{-1}([x_1]) = \{[ax_1 + t(x_3), x_3] \mid a \in \mathbf{k}^*, t \in \mathbf{k}[x_3]\}.$$

Let $h = (h_1, h_2, h_3) \in H_1 = \mathrm{Stab}(\pi^{-1}([x_1]))$. Since $h \in \mathrm{Stab}([x_3])$, we have $h_3 = \alpha x_3 + \beta$. Moreover, $h^{-1} \cdot [x_1, x_3] = [h_1, x_3]$, so $h_1 = ax_1 + t(x_3)$ for some $a \in \mathbf{k}^*$ and $t \in \mathbf{k}[x_3]$. Then we write $h_2 = \sum_{i \geqslant 0} c_i(x_1, x_3)x_2^i$, and compute the Jacobian of h, which must be a constant:

$$\mathrm{Jac}(h) = \begin{vmatrix} a & 0 & t'(x_3) \\ * & \sum_{i \geqslant 1} i\, c_i x_2^{i-1} & * \\ 0 & 0 & \alpha \end{vmatrix} = a\alpha \sum_{i \geqslant 1} i\, c_i x_2^{i-1}.$$

We obtain $c_1 \in \mathbf{k}^*$ and $c_i = 0$ for all $i \geqslant 2$, hence the expected expression $h_2 = dx_2 + P(x_1, x_3)$, where $P = c_0$ and $d = c_1$.

The proof for the form of elements $h = (h_1, h_2, h_3) \in H_2$ is in fact easier. Indeed, we have $[h_1, h_2] = [x_1, x_2]$ in $\mathcal{T}_{\mathbf{k}(x_3)}$ if and only if (h_1, h_2) is an element in the affine group over $\mathbf{k}(x_3)$, as desired. □

Using Lemma 3.3 and the classical theorem of Nagao [19, §1.6] about the amalgamated product structure of $\mathrm{GL}_2(\mathbf{k}[x_3])$, we obtain (proof left to the reader, see [2, Lem 4.8] for a very similar result):

LEMMA 3.4. – *We have*

$$H_2 = K_1 *_{K_1 \cap K_2} K_2,$$

where $K_2 = \left(\mathrm{GL}_2(\mathbf{k}) \ltimes \mathbf{k}[x_3]^2\right) \rtimes A_1$ *and* $K_1 = \left(\left\{\begin{pmatrix} a & 0 \\ c(x_3) & d \end{pmatrix}\right\} \ltimes \mathbf{k}[x_3]^2\right) \rtimes A_1.$

Finally, observing that $H_1 \cap H_2 = K_1$, and consequently $H_1 \cap K_2 = K_1 \cap K_2$, by combining Lemmas 3.2 and 3.4 we obtain an alternative decomposition of $\mathrm{Stab}([x_3])$:

PROPOSITION 3.5. – *We have*

$$\mathrm{Stab}([x_3]) = H_1 *_{H_1 \cap K_2} K_2.$$

Denote by $\mathscr{T}([x_3])$ the Bass-Serre tree of Proposition 3.5. Since K_2 is a supergroup in $\mathrm{Stab}([x_3])$ of the stabilizer of $[x_1, x_2, x_3]$, the tree $\mathscr{T}([x_3])$ admits a projection $\sigma : \mathscr{Z}([x_3]) \to \mathscr{T}([x_3])$ such that the following diagram commutes:

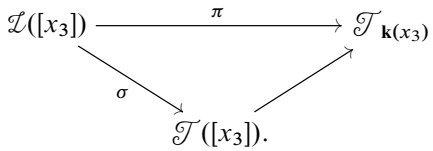

REMARK 3.6. – A type 3 vertex $v_3 \in \mathscr{Z}([x_3])$ satisfies $\sigma(v_3) = \sigma([x_1, x_2, x_3])$ if and only if $v_3 = [x_1 + t(x_3), x_2 + t'(x_3), x_3]$ for some $t, t' \in \mathbf{k}[x_3]$. Indeed, by definition v_3 is the image of $[x_1, x_2, x_3]$ under the action of an element of K_2. Since a representative of v_3 is defined up to an affine map, and $\mathrm{GL}_2(\mathbf{k}) \times A_1$ is a subgroup of the affine group A_3, we get the above form for v_3.

4. Diagrams and Curvature

A *disk diagram* $\mathscr{D}$ is a combinatorial (not necessarily simplicial) complex built of triangles, which is homeomorphic to a disk. A *disk diagram in* $\mathcal{C}$ is a combinatorial map of a disk diagram $\mathscr{D}$ into $\mathcal{C}$ (not necessarily an embedding). In that case a vertex of $\mathscr{D}$ has *type* i, if its image in $\mathcal{C}$ has type i. A disk diagram in $\mathcal{C}$ is *reduced*, if it is a local embedding at the interior points of edges and at interior vertices of type 1. We similarly define *reduced sphere diagrams*.

LEMMA 4.1. – *Each embedded loop in* $\mathcal{C}^1$ *bounds a reduced disk diagram.*

Proof. – By [13, Prop 5.7], the complex $\mathcal{C}$ is simply connected. Thus by [11, Lemma 1.6], there is a disk diagram $\mathcal{D} \to \mathcal{C}$ with prescribed $\partial\mathcal{D}$. Moreover, if $\mathcal{D}$ has minimal area, then it is automatically simplicial and $\mathcal{D} \to \mathcal{C}$ is a local embedding at edges. Finally, to obtain that $\mathcal{D} \to \mathcal{C}$ is a local embedding at interior type 1 vertices, it suffices to perform the following operation on $\mathcal{D}$. For each type 1 vertex v in $\mathcal{D}$ with edges $e_1, \dots, e_n$ starting at v that are mapped to the same edge of type $(1, i)$ in $\mathcal{C}$, we cut $\mathcal{D}$ along $e_1 \cup \cdots \cup e_n$ and reglue the arising $2n$-gon so that all type i vertices become identified. Repeating this operation finitely many times and keeping the notation $\mathcal{D}$ for the reglued disk, we obtain that $\mathcal{D} \to \mathcal{C}$ is reduced. Note that $\mathcal{D}$ is still a topological disk, since we assumed that $\partial\mathcal{D}$ embeds. □

4.1. Arrows

Let $\mathcal{D} \to \mathcal{C}$ be a reduced disk diagram in $\mathcal{C}$. Let T, T' be triangles in $\mathcal{D}$ with a common edge e of type $(1, 2)$. We will now describe, when do we equip this edge with an arrow (an orientation). We require the definition to be Tame($\mathbf{k}^3$)-equivariant and translate T, T' to the following pair.

LEMMA 4.2 (See [13, Cor 1.5]). – *Two triangles in $\mathcal{C}$ adjacent along an edge of type* $(1, 2)$ *can be sent by an element of* Tame($\mathbf{k}^3$) *to*

$$T = [x_1, x_2, x_3], [x_2, x_3], [x_3]$$
$$T' = [x_1 + P(x_2, x_3), x_2, x_3], [x_2, x_3], [x_3],$$

with $P \in \mathbf{k}[x_2, x_3]$ of degree at least 2.

In the situation of Lemma 4.2, if there exists a vertex $v_1 = [f(x_2, x_3)] \in \mathcal{T}([x_2, x_3])$ and a polynomial $A(X) \in \mathbf{k}[X]$ such that $P(x_2, x_3) = A(f(x_2, x_3))$, we say that the common edge e between T and T' is *oriented*. By Lemma 3.1(1), we know that P has the following form:

$$P(x_2, x_3) = c(ax_2 + bx_3)^d + \text{ lower order terms.}$$

To specify the orientation, we put an *arrow* on the edge e pointing towards the connected component of $\mathcal{T}_{[x_2,x_3]} - e$ containing $[ax_2 + bx_3]$ (see Figure 2). Note that by Lemma 3.1(1) that component contains also v_1.

Moreover, if P is a polynomial in x_3 (up to a linear term in x_2), then we say that the arrow on e is *terminal* and use a double arrow in figures. However, in future figures a single arrow might also represent a terminal one. If e is nonoriented, we use a wavy edge in figures.

REMARK 4.3. – In the definition of orientation, we do not claim that v_1 is unique, or that there is a unique way to write $P(x_2, x_3) = A(f(x_2, x_3))$. Indeed, consider the following example, where $d \geqslant 2$:

$$T' = [x_1 + x_2 + x_3^d, x_2, x_3], [x_2, x_3], [x_3]$$
$$= [x_1 + x_3^d, x_2, x_3], [x_2, x_3], [x_3].$$

One can treat T' as $[x_1 + A(f), x_2, x_3], [x_2, x_3], [x_3]$ in two ways:

$$\text{either } A(X) = X, \qquad f = x_2 + x_3^d;$$
$$\text{or } A(X) = X^d, \qquad f = x_3.$$

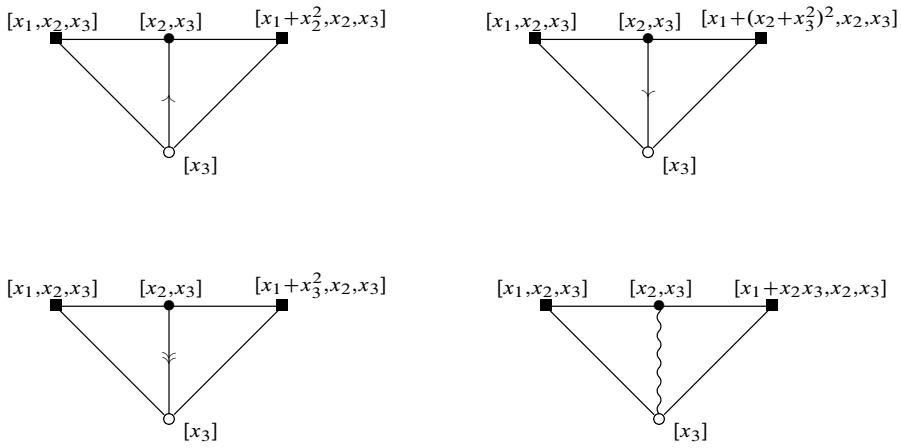

FIGURE 2. Examples of arrows

However, the leading term of $A(f)$ is uniquely defined, independently of such a choice.

LEMMA 4.4. – *Let $T = v_1, v_2, v_3$ and $T' = v_1, v_2, v_3'$ be two triangles in $\mathscr{D}$ adjacent along an edge of type* $(1,2)$. *Consider the map $\sigma\colon \mathscr{L}(v_1) \to \mathscr{T}(v_1)$ defined in Section 3. Then there is a terminal arrow from v_2 to v_1 if and only if $\sigma(v_3) = \sigma(v_3')$.*

Proof. – By Lemma 4.2, we can assume that $v_1 = [x_3]$, $v_2 = [x_2, x_3]$, $v_3 = [x_1, x_2, x_3]$, and $v_3' = [x_1 + P(x_2, x_3), x_2, x_3]$. By Remark 3.6, $\sigma(v_3) = \sigma(v_3')$ means that $P \in \mathbf{k}[x_3]$ (up to a linear term in x_2), which is precisely the definition of a terminal arrow. □

4.2. Curvature

In this subsection we define the *curvature* at each vertex of a reduced disk diagram $\mathscr{D}$ in $\mathcal{C}$.

First we consider an interior vertex v_i of $\mathscr{D}$. By $\deg v_i$ we denote its valence in $\mathscr{D}$, and by $\operatorname{out} v_i$ and $\operatorname{in} v_i$ the number of outgoing and incoming arrows (a terminal arrow is only counted once). The definition of the curvature $K(v_i)$ depends on the type i of the vertex:

$$K(v_1) = \frac{1}{12}(12 - \deg v_1) + \frac{\operatorname{out} v_1 - \operatorname{in} v_1}{6},$$
$$K(v_2) = \frac{1}{4}(4 - \deg v_2) + \frac{\operatorname{out} v_2 - \operatorname{in} v_2}{6},$$
$$K(v_3) = \frac{1}{6}(6 - \deg v_3).$$

One should imagine the triangles of $\mathcal{C}$ being equipped with angles $\frac{\pi}{6}, \frac{\pi}{2}, \frac{\pi}{3}$ with a correction coming from the arrows.

REMARK 4.5. – The valence of v_i is always even. Hence if $K(v_i)$ is negative, then in fact $K(v_i) \leqslant -\frac{1}{6}$.

Similarly we define the boundary curvature $K_\partial(v_i)$ of a boundary vertex v_i:

$$K_\partial(v_1) = \frac{1}{12}(7 - \deg v_1) + \frac{\operatorname{out} v_1 - \operatorname{in} v_1}{6},$$
$$K_\partial(v_2) = \frac{1}{4}(3 - \deg v_2) + \frac{\operatorname{out} v_2 - \operatorname{in} v_2}{6},$$
$$K_\partial(v_3) = \frac{1}{6}(4 - \deg v_3).$$

REMARK 4.6. – For $i = 2, 3$, the boundary curvature $K_\partial(v_i)$ is maximal when v_i has valence 2, giving $K_\partial(v_i) \leqslant \frac{1}{3}$. For $i = 1$, note that only every other additional edge might have an outgoing arrow. Hence the contribution $\frac{1}{6}$ from the out term of such an edge is canceled with the contribution $-2\frac{1}{12}$ from the deg term. Thus $K_\partial(v_1)$ is maximal when $\deg v_1 = 2k + 1$ and $\operatorname{out} v_1 = k$ giving $K_\partial(v_1) \leqslant \frac{1}{2}$.

As in classical small cancelation (see [15, Thm V.3.1]), we obtain the following.

PROPOSITION 4.7. – *(Combinatorial Gauss-Bonnet) For any reduced disk diagram $\mathcal{D}$ in $\mathcal{C}$, the sum of the curvatures and boundary curvatures of its vertices equals* 1. *Similarly, for any reduced sphere diagram in $\mathcal{C}$, the sum of the curvatures of its vertices equals* 2.

Proof. – First of all, since the out and the in terms cancel out in the summation, it suffices to prove the theorem when, in the definition of the curvature, these terms are omitted. Denote by w_i, e_{ij}, f the numbers of vertices of type i, edges of type (i, j), and faces in $\mathcal{D}$. The Euler characteristic of $\mathcal{D}$ can be expressed as

$$1 = w_1 + w_2 + w_3 - e_{12} - e_{13} - e_{23} + f$$
$$= \Big(w_1 - \frac{6(e_{12} + e_{13})}{12} + \frac{5f}{12}\Big) + \Big(w_2 - \frac{2(e_{12} + e_{23})}{4} + \frac{f}{4}\Big) + \Big(w_3 - \frac{3(e_{13} + e_{23})}{6} + \frac{2f}{6}\Big).$$

We claim that each of these terms can be recognized as the sum of the curvatures and boundary curvatures at the vertices of given type. Indeed, let V_1 be the set of all vertices of type 1 in $\mathcal{D}^0$. For each $v \in V_1$, let e^v, f^v be the number of edges and faces incident to v. If v is interior, then $K(v) = 1 - \frac{\deg v}{12}$ after ignoring the out and the in terms. Thus

$$K(v) = 1 - \frac{6 \deg v}{12} + \frac{5 \deg v}{12} = 1 - \frac{6e^v}{12} + \frac{5f^v}{12}.$$

If $v \in \partial\mathcal{D}$, we have $K_\partial(v) = 1 - \frac{\deg v}{12} - \frac{5}{12}$, and thus we obtain the same formula

$$K_\partial(v) = 1 - \frac{6 \deg v}{12} + \frac{5(\deg v - 1)}{12} = 1 - \frac{6e^v}{12} + \frac{5f^v}{12}.$$

Moreover, we have $\sum_{v \in V_1} e^v = e_{12} + e_{13}$ and $\sum_{v \in V_1} f^v = f$. This proves the claim for the vertices of type 1. The other types are dealt with similarly. The claim immediately implies the proposition. The sphere case follows in the same way. □

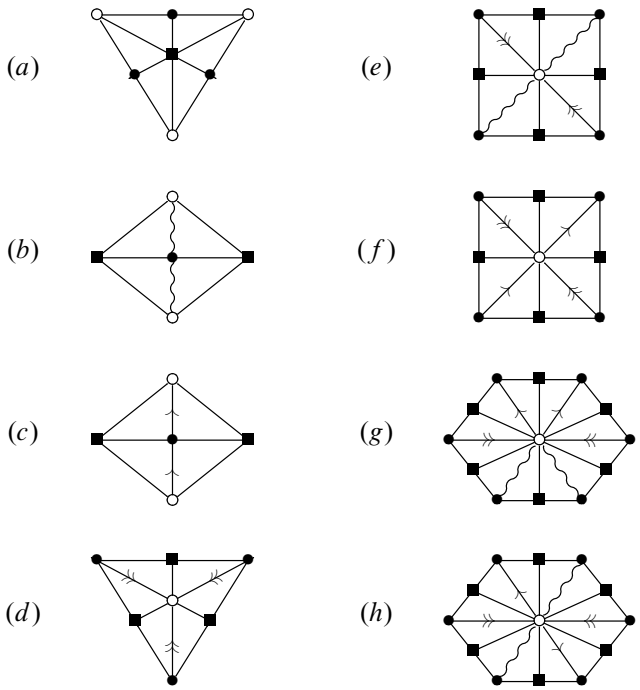

FIGURE 3. The eight cases of Proposition 5.1

5. Nonpositive curvature

In this section we study the curvature at interior vertices of reduced disk diagrams in $\mathcal{C}$, and in particular we prove Theorem A.

PROPOSITION 5.1. – *The curvature at an interior vertex of a reduced disk diagram is nonpositive, and equal to zero only in one of the eight situations in Figure 3.*

An arrow shown standard in Figure 3 is allowed to be terminal, and the edges on the boundary of the diagrams in Figure 3(a) might or might not carry arrows.

REMARK 5.2. – In each of the diagrams in Figure 3(d,e,f,g,h), given any 3 consecutive edges of type $(1, 2)$ from the central vertex, at least one carries an incoming arrow.

REMARK 5.3. – Among the diagrams in Figure 3(d,e,f,g,h), only in cases (g,h) there are two edges from the central vertex carrying outgoing arrows, and their distance in its link is 2 or 6 (and not 4).

To prove Proposition 5.1 we need the following preparatory lemmas.

LEMMA 5.4. – *There is no reduced disk diagram as in Figure 4(a).*

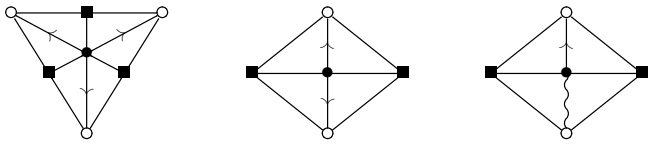

(*a*) (*b*) (*c*)

FIGURE 4. Three impossible cases around a type 2 vertex

Proof. – By contradiction, assume that such a diagram exists. Using the action of Tame($\mathbf{k}^3$) we can assume that the central vertex of the diagram is $[x_2, x_3]$, the three type 1 vertices are $[x_2]$, $[x_3]$ and $[x_2 + x_3]$, and one of the type 3 vertices is $[x_1, x_2, x_3]$. Then the arrows imply that the remaining type 3 vertices have the form $[x_1 + A(f), x_2, x_3]$ and $[x_1 - B(g), x_2, x_3]$, with a relation of the form

$$A(f) + B(g) = C(h), \tag{1}$$

for some components $f, g, h \in \mathbf{k}[x_2, x_3]$ and some polynomials $A, B, C \in \mathbf{k}[X]$. By Lemma 3.1(1), we know that the leading monomials of $A(f)$, $B(g)$ and $C(h)$ have the form x_2^a, x_3^b, $(x_2 + x_3)^c$. Moreover, since the type 3 vertices are distinct, we have $a, b, c \geqslant 2$. This is incompatible with relation (1). □

LEMMA 5.5. – *There are no reduced disk diagrams as in Figure 4(b,c).*

Proof. – We can suppose that the central vertex v_2 of the diagram is $[x_2, x_3]$ and that its type 3 neighbors are $[x_1, x_2, x_3]$ and $[x_1 + P(x_2, x_3), x_2, x_3]$. Let e be an edge from v_2 with an outgoing arrow, and let e' be the other type $(1, 2)$ edge (possibly also with an arrow). Since e is oriented, there is a type 1 vertex $v_1 = [f(x_2, x_3)]$ with $P = A(f)$. Since the two triangles containing e' differ also by $[x_1, x_2, x_3]$ and $[x_1 + P(x_2, x_3), x_2, x_3]$, the edge e' is also oriented and the arrows on e, e' in $\mathscr{T}(v_2)$ point both towards v_1. This excludes the diagrams in Figure 4(b,c). □

In the following lemma we discuss configurations in the link of a type 1 vertex v_1 with a specified image in $\mathscr{T}(v_1)$ under σ from Section 3.

LEMMA 5.6. – (a) *In a reduced disk diagram as in Figure 5(a), if the left horizontal edge has an arrow outgoing from the central vertex, then the other horizontal edge has an incoming arrow.*

(b) *There is no reduced disk diagram with a type 1 vertex v_1 that has a pair of disjoint length 2 paths in the link mapping to the same length 2 path in $\mathscr{T}(v_1)$, and equipped with a pair of arrows as in Figure 5(b).*

Note that the terminal arrows in Figure 5(a) come from Lemma 4.4.

Proof. – Let $v_2 = [x_2, x_3]$. In both cases we can assume that the seven central vertices are labeled as in Figure 6, with $[f(x_2, x_3)] \in \mathscr{T}(v_2)$ and A, P, Q, R polynomials in one variable (here we use Remark 3.6 that characterizes vertices with the same image under σ).

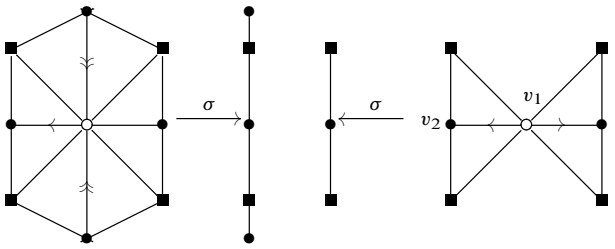

FIGURE 5.

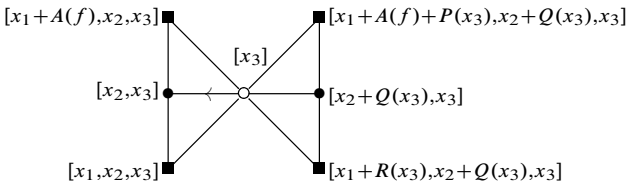

FIGURE 6.

1. The existence of a vertex of type 2 between $[x_1 + A(f) + P(x_3), x_2 + Q(x_3), x_3]$ and $[x_1 + A(f), x_2, x_3]$, and the fact that $\deg Q \geqslant 2$ (otherwise the left and right type 2 vertices would not be distinct) imply $\deg P \leqslant 1$. So up to changing the representative we can assume that $P = 0$, and by a symmetric argument $R = 0$. Then the right horizontal edge is oriented in $\mathscr{T}(v_2)$ towards the vertex $[f]$, as is the left horizontal edge, to the left.

2. We can further assume that the first type 1 vertex on the path from $[x_3]$ to $[f]$ in $\mathscr{T}(v_2)$ is $[x_2]$. Then by Lemma 3.1(1)(and the fact that the vertices $[x_1, x_2, x_3]$ and $[x_1 + A(f), x_2, x_3]$ are distinct, hence $\deg A(f) \geqslant 2$), there exists $d \geqslant 2$ such that the leading monomial of $A(f)$ is cx_2^d.

Since the right horizontal edge is oriented, there exist a polynomial $B \in \mathbf{k}[X]$ and a component $g \in \mathbf{k}[x_2 + Q(x_3), x_3] = \mathbf{k}[x_2, x_3]$ such that

$$A(f) + B(g) + (P - R)(x_3) = 0. \tag{2}$$

The right horizontal edge is oriented to the right, and towards $[g]$ in $\mathscr{T}(v_2)$, so $[g] \neq [x_3]$ lies in the component of $\mathscr{T}(v_2) - v_2$ containing $[x_3]$. Consequently, by Lemma 3.1(2), there exists $d' \geqslant 0$ such that the terms in $B(g)$ of degree greater than d' have the form $H(x_3)x_3^{d'+1} + c'x_2x_3^{d'}$ for some nonconstant H.

So either $d > d'$ and the monomial cx_2^d from $A(f)$ cannot be canceled out by any other term in (2), or $d' + 1 > d$ and the same remark applies to the monomial $c'x_2x_3^{d'}$ from $B(g)$, leading to a contradiction in both cases. □

Proof of Proposition 5.1. – Since the link of a vertex v_3 of type 3 is the incidence graph of a projective plane, its minimal length immersed loop has length 6. Thus $K(v_3) \leqslant 0$ with the only equality case being Figure 3(a).

Consider now a vertex v_2 of type 2. Recall that its link $\mathscr{L}(v_2)$ is a (complete) bipartite graph. If $\deg v_2 = 2n \geqslant 8$, then

$$K(v_2) = \frac{1}{4}(4 - \deg v_2) + \frac{\operatorname{out} v_2 - \operatorname{in} v_2}{6} \leqslant 1 - 2n\frac{1}{4} + n\frac{1}{6} = 1 - \frac{n}{3} < 0.$$

In the case where $2n = 6$, in order to obtain $K(v_2) < 0$, we need to exclude the situation where there are three outgoing arrows from v_2. This is exactly Lemma 5.4. Finally, if $2n = 4$, we have $K(v_2) = \frac{\operatorname{out} v_2 - \operatorname{in} v_2}{6}$. By Lemma 5.5, if there is an outgoing arrow from v_2, there is also an incoming arrow to v_2. Thus $K(v_2) \leqslant 0$ with the only equality cases in Figure 3(b,c).

Finally consider a vertex v_1 of type 1 with $\deg v_1 = 2n$. Let γ be the corresponding length $2n$ loop in $\mathscr{L}(v_1)$. Since $\mathscr{D}$ is reduced, γ is embedded. For each pair of vertices of type 3 at distance 2 in $\mathscr{L}(v_1)$ there is only one length 2 path joining them. Hence $2n \geqslant 6$. We have $K(v_1) = \frac{1}{6}(6 - n) + \frac{\operatorname{out} v_1 - \operatorname{in} v_1}{6}$. Denote by $\operatorname{non} v_1$ the number of nonoriented edges among the n type $(1,2)$ edges incident to v_1. Since $n = \operatorname{non} v_1 + \operatorname{out} v_1 + \operatorname{in} v_1$, we have

$$K(v_1) = \frac{1}{6}\big(6 - \operatorname{non} v_1 - 2\operatorname{in} v_1\big).$$

Consider the projection $\sigma \circ \gamma$ in the tree $\mathscr{T}(v_1)$ from Proposition 3.5. Note that at each type 3 vertex in $\mathscr{L}(v_1)$, the projection σ is a local embedding. If the number of vertices at which $\sigma \circ \gamma$ is not a local embedding (i.e., the number of backtracks in the tree $\mathscr{T}(v_1)$) is at least 3, then by Lemma 4.4, we have $\operatorname{in} v_1 \geqslant 3$. Consequently $K(v_1) \leqslant 0$. If $K(v_1) = 0$, then $\operatorname{in} v_1 = 3$, so $\sigma \circ \gamma$ is a tripod. Moreover, since $\operatorname{non} v_1 = 0$, by Lemma 5.6(b) all the tripod legs have length 1, so $n = 3$ as in Figure 3(d). It remains to consider the case where $\sigma \circ \gamma$ is not a local embedding only at 2 vertices. In particular, its image is an embedded path of even length n, containing $\frac{n}{2} - 1$ length 2 paths to which we can apply Lemma 5.6(b). If $K(v_1) \geqslant 0$, then $\operatorname{non} v_1 \leqslant 2$. Then by Lemma 5.6(b) we have $n \leqslant 6$. Moreover, if $n = 6$, then we are in one of the cases of Figure 3(g,h). It remains to consider the case where $n = 4$. To arrive at Figure 3(e,f), we need to prove that if there is an outgoing arrow from v_1, then the opposite edge of type (1,2) from v_1 is equipped with an incoming arrow. This is exactly Lemma 5.6(a). □

As a consequence we now obtain the contractibility of the complex $\mathcal{C}$.

Proof of Theorem A. – By [13, Prop 5.7], the complex $\mathcal{C}$ is simply connected. Since $\mathcal{C}$ is 2-dimensional, by Whitehead and Hurewicz theorems, it suffices to show that $\pi_2(\mathcal{C})$ is trivial. Otherwise, using the same operation as in the proof of Lemma 4.1, we find a reduced sphere diagram in $\mathcal{C}$. All its vertices are interior and by Proposition 5.1 they all have nonpositive curvature. This contradicts Proposition 4.7. □

6. Hyperbolicity

In this section we prove Theorem B. We will appeal to the following criterion for Gromov-hyperbolicity.

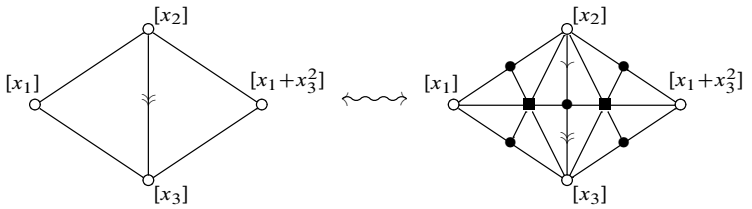

FIGURE 7. Example of a directed edge in a simplified diagram with only type 1 vertices

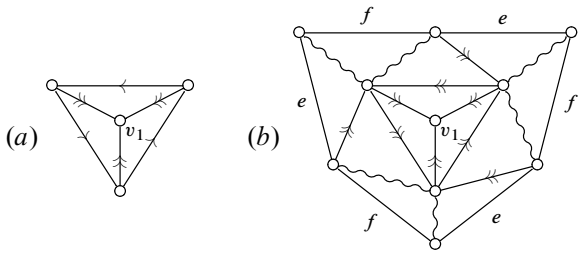

FIGURE 8. Case $v_1 \in Z_6$

PROPOSITION 6.1. – *Let X be a simplicial complex. Suppose that there exist constants C, C', such that for each combinatorial loop γ of length l embedded in X there is a disk diagram $\mathscr{D} \to X$ with $\partial\mathscr{D} = \gamma$ and a set $N \subset D^0$ of cardinality $\leqslant Cl$ such that the C'-neighborhoods in $\mathscr{D}^1$ around $\partial\mathscr{D} \cup N$ cover the entire $\mathscr{D}$. Then X is Gromov-hyperbolic.*

The proof is routine and we postpone it to the end of the section.

Proof of Theorem B. – For each combinatorial loop γ of length l embedded in $\mathcal{C}$, consider a reduced disk diagram $\mathscr{D} \to \mathcal{C}$ with $\partial\mathscr{D} = \gamma$ (guaranteed by Lemma 4.1). Let $N \subset \mathscr{D}^0$ be the set of interior vertices of $\mathscr{D}$ with negative curvature. Each vertex in N has curvature $\leqslant -\frac{1}{6}$ by Remark 4.5. Furthermore, for each boundary vertex of $\mathscr{D}$, its boundary curvature is $\leqslant \frac{1}{2}$ by Remark 4.6. Thus by Proposition 4.7, we have $|N| \leqslant 3l$, so we can take $C = 3$. We will prove that $C' = 11$ satisfies the hypothesis of Proposition 6.1.

Let $Z \subset \mathscr{D}^0$ be the set of interior type 1 vertices with zero curvature. By Proposition 5.1, we have $Z = Z_6 \cup Z_8 \cup Z_{12}$, where Z_n denotes the subset of vertices in Z with valence n. We will prove that each vertex $v_1 \in Z$ lies at distance $\leqslant 10$ from $\partial\mathscr{D} \cup N$. So let us assume by contradiction that there exists $v_1 \in Z$ with no vertex in $\partial\mathscr{D} \cup N$ at distance $\leqslant 10$ from v_1. Let $F \subset \mathscr{D}$ (for 'Flat') be the union of all the triangles of $\mathscr{D}$ with their vertices at distance $\leqslant 10$ in $\mathscr{D}^1$ from v_1. Then by Proposition 5.1, all interior vertices of F of type 2 and 3 have valences 4 and 6, respectively. In the figures of F (or subdiagrams of F) that follow, we can thus combine the 6 triangles of F around each type 3 vertex to obtain a triangulation of F with only type 1 vertices. Here an arrow between two vertices of type 1 means two successive arrows, and a terminal arrow means that the second arrow is terminal: see Figure 7. Observe also that in these simplified diagrams the valence of each type 1 vertex is half the original one.

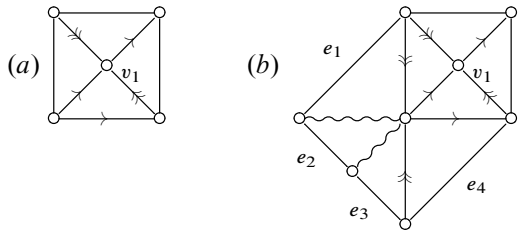

FIGURE 9. Case $v_1 \in Z_8$, subcase (f)

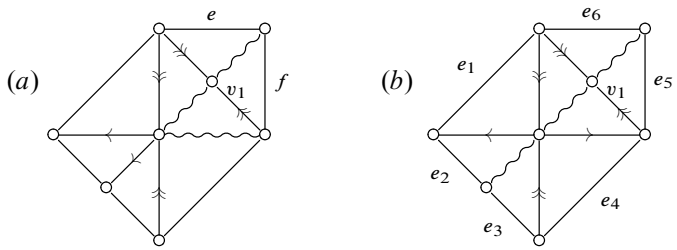

FIGURE 10. Case $v_1 \in Z_8$, subcase (e)

First consider the case where $v_1 \in Z_6$, corresponding to Figure 3(d). By Remark 5.2, the boundary edges of the three triangles containing v_1 must carry arrows, say counterclockwise as in Figure 8(a) (the clockwise case is analogous). Around the non-central type 1 vertices, we have two consecutive outgoing arrows, so the only possible configuration is Figure 3(g), and we obtain Figure 8(b) as a subset of the flat neighborhood F. By Remark 5.2, the edges labeled e must be oriented counterclockwise. Then applying again Remark 5.2 to both endpoints of the edges labeled f forces them to be oriented at the same time clockwise and counterclockwise, a contradiction. Thus each $v_1 \in Z_6$ is at distance $\leqslant 4$ from $\partial\mathscr{D} \cup N$.

Consider now $v_1 \in Z_8$, that is, we are in one of the two cases of Figure 3(e,f).

First consider case (f), see Figure 9. Analyzing the configuration at the top right vertex, by Remark 5.3 we cannot simultaneously have the top edge oriented leftwards and the right edge oriented downwards. Thus by Remark 5.2 applied to the top left and the bottom right vertex, without loss of generality the bottom edge is oriented rightwards, as in Figure 9(a). Then with two consecutive outgoing arrows the bottom left vertex must correspond to Figure 3(g), see Figure 9(b). Applying four times Remark 5.2, we obtain successively that the edges e_1, e_2, e_3, e_4 are all oriented clockwise. Then Remark 5.3 gives a contradiction from the point of view of the right bottom vertex. Thus each $v_1 \in Z_8$ corresponding to case (f) is at distance $\leqslant 4$ from $\partial\mathscr{D} \cup N$.

We continue with case (e). If the bottom left vertex is also of the form (e), we replace v_1 with this vertex and observe that now the new bottom left vertex is not of the form (e) anymore. Indeed, otherwise the top left and bottom right vertices would have three consecutive outgoing arrows contradicting Remark 5.2. So after at most one such replacement the bottom left vertex is of the form (g) or (h).

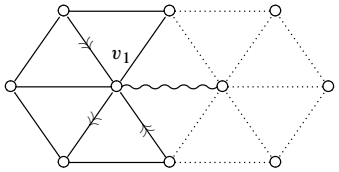

FIGURE 11. Case $v_1 \in Z_{12}$

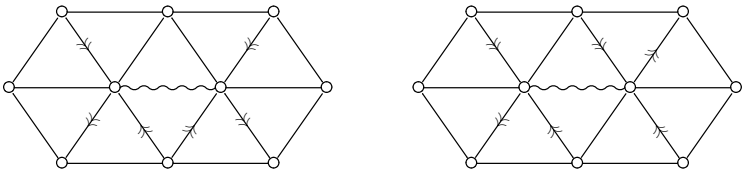

(a) (b)

FIGURE 12. Forbidden bihexagonal diagrams

On the one hand, if it is of the form (g), as in Figure 10(a), then by Remark 5.2, the edges e and f are both oriented away from the top right vertex. But this contradicts Remark 5.2 at that vertex.

On the other hand, if the bottom left vertex is of the form (h), as in Figure 10(b), by applying Remark 5.2 we obtain successively that e_1 is oriented clockwise, and e_6, e_5 are oriented counterclockwise. Then the common vertex of e_4 and e_5 admits two consecutive outgoing arrows, hence must correspond to case (g) of Figure 3, and thus e_4 is nonoriented. Applying Remark 5.2 again we get that e_3, e_2 are oriented counterclockwise. By Remark 5.3 this is not possible from the point of view of the common vertex of e_1 and e_2.

Given that we might have replaced v_1 at the beginning of the discussion, this shows that each $v_1 \in Z_8$ in case (e) is at distance $\leqslant 6$ from $\partial\mathscr{D} \cup N$.

Finally, let us consider $v_1 \in Z_{12}$. We now prove that v_1 is at distance $\leqslant 4$ from $Z_6 \cup Z_8 \cup \partial\mathscr{D} \cup N$. Otherwise, the configurations at all type 1 vertices at distance $\leqslant 4$ from v_1 are as in Figure 3(g,h). In particular up to symmetry we are in the situation of Figure 11, where all type 1 vertices are of type (g) or (h), which gives that all arrows in sight are terminal. There are two possibilities for the two incoming arrows in the dotted hexagon on the right, which lead to the two excluded diagrams of the following final Lemma 6.2.

This proves that any type 1 vertex of $\mathscr{D}$ is at distance $\leqslant 4 + 6 = 10$ from $\partial\mathscr{D} \cup N$ and consequently, any vertex of $\mathscr{D}$ is at distance $\leqslant 11$ from $\partial\mathscr{D} \cup N$. □

LEMMA 6.2. – *There are no reduced disk diagrams as in Figure 12, (a) or (b).*

Proof. – For Figure 12(a), using the action of the group $\mathrm{Tame}(\mathbf{k}^3)$, we can make the choice of representatives as in Figure 13, where $A, B, C, D \in \mathbf{k}[X]$ are polynomials of degree at least 2. Moreover, there exist polynomials $E, F \in \mathbf{k}[X]$, also of degree at least 2, such that

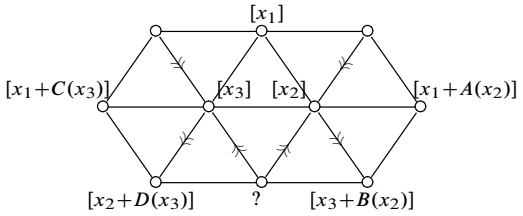

FIGURE 13.

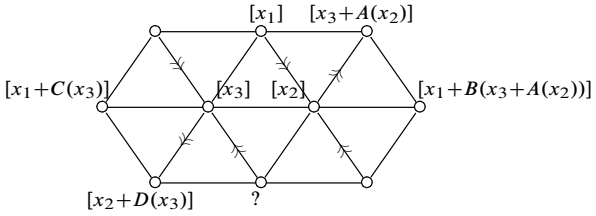

FIGURE 14.

the central bottom vertex has the form

$$[x_1 + A(x_2) + E(x_3 + B(x_2))] = [x_1 + C(x_3) + F(x_2 + D(x_3))].$$

By computing the second-order derivative $\frac{\partial^2}{\partial x_2 \partial x_3}$ on both sides we obtain

$$B'(x_2)E''(x_3 + B(x_2)) = D'(x_3)F''(x_2 + D(x_3)),$$

which is impossible in view of the monomials of highest degrees.

Similarly in the situation of Figure 12(b) we can choose representatives as in Figure 14. Then there exist polynomials $E, F \in \mathbf{k}[X]$ such that the central bottom vertex has the form

$$[x_1 + E(x_2) + B(x_3 + A(x_2))] = [x_1 + C(x_3) + F(x_2 + D(x_3))],$$

and we get a contradiction as in the previous case. □

Proof of Proposition 6.1. – By [4, Thm III.H.2.9], via Definitions 2.1, and Remarks 2.3 (1,2,5) therein, to prove that $\mathcal{C}$ is Gromov-hyperbolic it suffices to show that any combinatorial loop γ embedded in $\mathcal{C}$ is the boundary loop of a following triangulated disk $T \to \mathcal{C}$. First of all, we require that $|T^0|$ is linear in $|\gamma|$. Secondly, we require that adjacent vertices in T^0 are sent to vertices in $\mathcal{C}^0$ at a uniformly bounded distance. The map $T \to \mathcal{C}$ does not need to be combinatorial (or even continuous).

To find such T, let $\mathscr{D}$ be the disk diagram with boundary γ guaranteed by the hypothesis. For each vertex v of $\mathscr{D}$ outside $N \cup \partial\mathscr{D}^0$ choose an edge $e(v)$ joining v to a vertex closer to $N \cup \partial\mathscr{D}^0$ in $\mathscr{D}^1$. Combine the triangles of the barycentric subdivision $\mathscr{D}'$ of $\mathscr{D}$ incident to a common vertex of $\mathscr{D}$ to form a combinatorial subdivision S of $\mathscr{D}$. Combine the cells of S containing vertices joined by some $e(v)$. Label each such combined cell s by the unique vertex $v(s) \in N \cup \partial\mathscr{D}^0$ that it contains. By the hypothesis, any vertex in such a cell is at distance $\leqslant C'$ in $\mathscr{D}^1$ from $v(s)$. If some cell s becomes non-simply connected, incorporate all the cells that it bounds into s. We thus obtain a combinatorial subdivision S' of $\mathscr{D}$ with

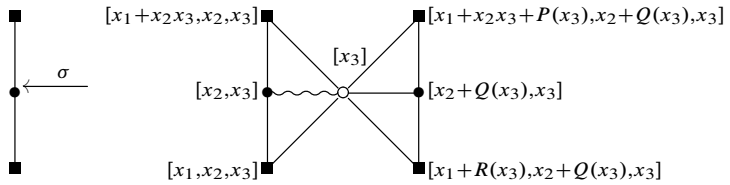

FIGURE 15. Here $P, Q, R \in \mathbf{k}[X]$ are arbitrary polynomials, so some of the vertices on the right and on the left might coincide

at most $|N \cup \partial \mathscr{D}^0| \leqslant Cl$ cells. Since at each vertex of S' there are exactly 3 cells meeting, consider the triangulation T dual to S' with vertices labeled $v(s)$. For each edge $v(s)v(s')$ of T, in the metric of $\mathscr{D}^1$ we have $|v(s), v(s')| \leqslant 2C' + 1$, as desired. □

7. Loxodromic WPD element

In this section we prove Theorems C and D. Recall that $g, h, f \in \mathrm{Tame}(\mathbf{k}^3)$ are of the form $g^{-1} = (x_2, x_1 + x_2x_3, x_3)$, $h^{-1} = (x_3, x_1, x_2)$, $f = g^n \circ h$, where $n \geqslant 0$. We now define a candidate axis γ for f.

DEFINITION 7.1. – Consider the following map $\gamma\colon \mathbb{R} \to \mathcal{C}^1$. Let $\gamma(0) = [x_1], \gamma(1) = [x_1, x_3], \gamma(2) = [x_3]$, and let $\gamma[0, 2]$ be the corresponding length 2 path. Note that $f \cdot \gamma(0) = [x_1 \circ f^{-1}] = [x_1 \circ h^{-1} \circ g^{-n}] = [x_3] = \gamma(2)$. We can thus extend the definition to $\gamma[2k, 2k + 2] = f^k \cdot \gamma[0, 2]$.

REMARK 7.2. – For any reduced disk diagram with $\gamma[0, 2]$ in the boundary, the boundary curvature at the type 2 vertex $\gamma(1)$ is nonpositive, since there are at least 3 nonoriented edges from $\gamma(1)$: two boundary edges and one of type $(2, 3)$.

We shall need the following technical lemma, which is similar to Lemma 5.6.

LEMMA 7.3. – *In the situation of Figure 15, the horizontal edge on the right is nonoriented.*

Proof. – Assume the right horizontal edge is oriented. Then there exist a component $\phi(x_2, x_3) \in \mathbf{k}[x_2, x_3] = \mathbf{k}[x_2 + Q(x_3), x_3]$ and a polynomial $A(X) \in \mathbf{k}[X]$ such that

$$x_2x_3 + (P - R)(x_3) + A(\phi) = 0.$$

Comparing degrees in x_2 we must have $\deg_{x_2} \phi = 1$ and $\deg A = 1$, so that $A(\phi)$ has the form

$$A(\phi) = ax_2 + S(x_3).$$

But then $A(\phi)$ contains no terms canceling out with x_2x_3, contradiction. □

We now establish the key result towards the proof that $f = g^n \circ h$ is a loxodromic WPD element, which is an analog of Remark 7.2 for a type 1 vertex.

PROPOSITION 7.4. – *Let $\mathscr{D} \to \mathcal{C}$ be any reduced disk diagram that agrees on a subpath of $\partial \mathscr{D}$ with $\gamma[1, 3]$. Then the boundary curvature at $\gamma(2)$ is $\leqslant \frac{2-n}{6}$.*

Proof. – Denote by in, out, and non the number of type (1,2) edges incident to $\gamma(2)$ in $\mathscr{D}$ that carry incoming, outgoing, or no arrows, respectively. Since $\gamma(1), \gamma(3)$ are both of type 2, the valence of $\gamma(2)$ in $\mathscr{D}$ equals $2(\text{in}+\text{out}+\text{non})-1$. Thus the boundary curvature at $\gamma(2)$ is

$$K_\partial(\gamma(2)) = \frac{1}{12}\Big(7 - 2(\text{in} + \text{out} + \text{non}) + 1\Big) + \frac{\text{out} - \text{in}}{6} = \frac{4 - 2\text{in} - \text{non}}{6}.$$

The two boundary edges do not carry arrows by definition. Thus to prove the proposition it suffices to find n other edges, either nonoriented or with an incoming arrow (in the following estimate, we do not try to take advantage of the fact that the incoming arrows have a coefficient 2 in the above formula).

Observe that

$$\gamma(3) = f \cdot \gamma(1) = (g^n \circ h) \cdot [x_1, x_3] = g^n \cdot [x_2, x_3].$$

In the link $\mathscr{L}([x_3])$ of $[x_3]$, let e_0^- be the edge from $[x_1, x_3]$ to $[x_1, x_2, x_3]$ and let e_0^+ be the edge from $[x_1, x_2, x_3]$ to $[x_2, x_3]$. For $k = 1, \dots, n$, let $e_k^- = g^k \cdot e_0^-$ and $e_k^+ = g^k \cdot e_0^+$. Since $g \cdot [x_1, x_3] = [x_2, x_3]$, we have that $\delta = e_0^- e_0^+ e_1^- e_1^+ \cdots e_n^- e_n^+$ is a path from $\gamma(1)$ to $\gamma(3)$.

We will now use the projection $\sigma\colon \mathscr{L}([x_3]) \to \mathscr{T}([x_3])$ from Proposition 3.5. Since e_1^- ends at $g \cdot [x_1, x_2, x_3] = [x_1 + x_2 x_3, x_2, x_3]$, we have that $\sigma(e_0^- e_0^+ e_1^-)$ is an embedded length 3 path in the tree $\mathscr{T}([x_3])$. Consequently $\sigma \circ \delta$ is a geodesic.

Let $\hat{\delta}$ be the link of $\gamma(2)$ in $\mathscr{D}$. It is an other path in $\mathscr{L}([x_3])$ from $\gamma(1)$ to $\gamma(3)$. Thus the path $\sigma \circ \hat{\delta}$ in $\mathscr{T}([x_3])$ has the same endpoints as the geodesic $\sigma \circ \delta$. Consequently, there are edges $\hat{e}_0^-, \hat{e}_0^+, \hat{e}_1^-, \dots, \hat{e}_n^+$ that appear in $\hat{\delta}$ in that order satisfying $\sigma(\hat{e}_k^\pm) = \sigma(e_k^\pm)$ for all $k = 0, \dots, n$.

Let $\tilde{\delta} \subset \hat{\delta}$ be the subpath between the endpoint of $\hat{e}_0^+$ and the starting point of $\hat{e}_1^-$. If $\tilde{\delta}$ is not a single vertex, then σ maps it to a closed path in $\mathscr{T}([x_3])$. Thus $\sigma \circ \tilde{\delta}$ is not a local embedding, and by Lemma 4.4 there exists a vertex v_2 in $\tilde{\delta}$ with a terminal arrow from v_2 to $\gamma(2)$ in $\mathscr{D}$. If $\tilde{\delta}$ is a single vertex v_2, then we obtain the configuration of Figure 15, where e_0^+, e_1^- are the vertical edges on the left, and $\hat{e}_0^+, \hat{e}_1^-$ are the vertical edges on the right. By Lemma 7.3, the edge from v_2 to $\gamma(2)$ is nonoriented.

Analogously one proves that for each $k = 1, \dots, n-1$, there is a vertex v_2 between the endpoint of $\hat{e}_k^+$ and the starting point of $\hat{e}_{k+1}^-$, with a terminal arrow or nonoriented edge from v_2 to $\gamma(2)$. □

Proof of Theorem C. – We will prove that for any $s < t \in \mathbb{Z}$, the distance between $\gamma(s)$ and $\gamma(t)$ is $> \lambda|t - s|$, where $\lambda = \frac{1}{6}$. Otherwise, let s, t take the closest values such that the above estimate is violated, and let α be a geodesic in $\mathcal{C}^1$ from $\gamma(t)$ to $\gamma(s)$. We claim that the loop $\gamma[s,t]\alpha$ is embedded. Indeed, if already $\gamma[s,t]$ self-intersected, then the maximal embedded interval $[s', t'] \subset [s, t]$ would also violate our estimate. Moreover, if α intersected $\gamma[s,t]$ in a point $\gamma(t')$, then either $[s, t']$ or $[t', t]$ would violate our estimate. This justifies the claim that $\gamma[s,t]\alpha$ is embedded.

Let $\mathscr{D}$ be a reduced disk diagram with boundary $\gamma[s,t]\alpha$. By Proposition 5.1, all the interior vertices of $\mathscr{D}$ have nonpositive curvature. By Remark 4.6, each vertex of α, including the endpoints, has boundary curvature $\leqslant \frac{1}{2}$, so the sum of their boundary curvatures is $\leqslant \frac{1}{2}(\lambda(t-s)+1)$. By Proposition 7.4, for every even integer $s < k < t$, the boundary

curvature at $\gamma(k)$ is $\leqslant -\frac{1}{6}$, and by Remark 7.2, the boundary curvature is nonpositive at odd integers. By Proposition 4.7, we obtain

$$1 \leqslant \frac{1}{2}(\lambda(t-s)+1) - \frac{1}{6}\Big(\frac{t-s}{2} - 1\Big).$$

After comparing the terms with and without $(t-s)$ this yields a contradiction. □

Along the proof we established the following.

COROLLARY 7.5. – *γ is embedded.*

For the proof of Theorem D, we need some preparatory lemmas.

LEMMA 7.6. – *Let $n \geqslant 12$ and let α be any geodesic in $\mathcal{C}^1$ with endpoints $\gamma(t), \gamma(s)$, where $s < t$, and with other vertices disjoint from γ. Then $t - s = 2$ and s, t are even.*

Proof. – Let $\mathscr{D}$ be a reduced disk diagram with boundary $\gamma[s,t]\alpha$. By Proposition 5.1, all the interior vertices of $\mathscr{D}$ have nonpositive curvature. By Remark 4.6, the sum of the boundary curvatures of the vertices of α is $\leqslant \frac{1}{2}(t-s+1) = (\frac{t-s}{2}-2)+\frac{5}{2}$. By Proposition 7.4, for every even integer $s < k < t$, the boundary curvature at $\gamma(k)$ is $\leqslant \frac{2-n}{6} < -\frac{3}{2}$. Assuming, by contradiction, that $t - s > 2$, or $t - s = 2$ and t, s are odd, we obtain that there exists such k. Together with Remark 7.2, this shows that the sum of the boundary curvatures at the interior vertices of $\gamma[s,t]$ is $< -\frac{3}{2}$.

Moreover, if $t - s \geqslant 4$, so $\frac{t-s}{2} - 2 \geqslant 0$, then the sum of the boundary curvatures at the interior vertices of $\gamma[s,t]$ is $< -\frac{3}{2} - \frac{3}{2}(\frac{t-s}{2} - 2)$. In that case by Proposition 4.7, we obtain $1 < (\frac{t-s}{2}-2)+\frac{5}{2}-\frac{3}{2}-\frac{3}{2}(\frac{t-s}{2}-2) \leqslant 1$, which is a contradiction. In the case where $t-s = 3$, or where $t - s = 2$ and t, s are odd, from Proposition 4.7 we obtain $1 < \frac{1}{2} \cdot 4 - \frac{3}{2}$, which is again a contradiction. □

We have the following immediate consequences.

COROLLARY 7.7. – *Let $n \geqslant 12$ and let α be any geodesic with endpoints $\gamma(t), \gamma(s)$. Then for any even k between s and t, the vertex $\gamma(k)$ lies in α.*

COROLLARY 7.8. – *For $n \geqslant 12$, γ is a geodesic.*

We continue with one more similar lemma.

LEMMA 7.9. – *Let $n \geqslant 12$ and $C \geqslant 1$. Suppose that $v, v' \in \mathcal{C}^0$ are at distance $\leqslant C$ from $\gamma(s), \gamma(t)$, respectively. Moreover, assume $|s-t| \geqslant 12C$. Then any geodesic from v' to v intersects γ.*

Proof. – We prove the lemma by contradiction. Suppose that v', v are as above with geodesic α between them disjoint from γ. Moreover, assume that the distance between v' and v is minimal possible. We can assume $s < t$. Let β, β' be geodesics between v and $\gamma(s)$, and $\gamma(t)$ and v'. Then the loop $\delta = \gamma[s,t]\beta'\alpha\beta$ is embedded, since otherwise we could replace one of v, v' by a vertex of self-intersection, decreasing the distance between v' and v.

Let $\mathscr{D} \to \mathcal{C}$ be a reduced disk diagram with boundary δ. By Proposition 5.1, all the interior vertices of $\mathscr{D}$ have nonpositive curvature. Since α is a geodesic, we have $|\alpha| \leqslant 2C + t - s$. Hence by Remark 4.6, the sum of the boundary curvatures at the vertices of $\beta'\alpha\beta$ is

$\leqslant \frac{1}{2}(4C+t-s+1)$. By Remark 7.2 and Proposition 7.4, the sum of the boundary curvatures at the interior vertices of $\gamma[s,t]$ is $\leqslant \frac{2-n}{6}\left(\frac{t-s}{2}-1\right) < -\frac{3}{4}\big((t-s)-2\big)$. By Proposition 4.7, we obtain

$$\begin{aligned} 1 &< \frac{1}{2}\Big(1+4C+(t-s)\Big) - \frac{3}{4}\Big((t-s)-2\Big) \\ &= \frac{1}{2} + 2C - \frac{1}{4}\big(t-s\big) + \frac{3}{2} \leqslant 2C - \frac{1}{4}12C + 2 \leqslant 2-1, \end{aligned}$$

which is a contradiction. □

Recall that we defined $g^{-1} = (x_2, x_1 + x_2x_3, x_3)$. We now compute the iterates of g.

LEMMA 7.10. – *There exist polynomials $P_n, Q_n \in \mathbf{k}[x_3]$ such that for any $n \geqslant 1$*

$$\begin{aligned} g^n &= (x_1Q_n(x_3) + x_2Q_{n-1}(x_3), x_1Q_{n-1}(x_3) + x_2Q_{n-2}(x_3), x_3), \\ g^{-n} &= (x_1P_{n-2}(x_3) + x_2P_{n-1}(x_3), x_1P_{n-1}(x_3) + x_2P_n(x_3), x_3). \end{aligned}$$

Moreover P_n, Q_n is an odd (resp. even) polynomial if n is odd (resp. even), and $P_n(0) = Q_n(0) = 1$ for any even n.

Proof. – The existence of the polynomials follows from the fact that we can view $g^{\pm 1}$ as elements of $\mathrm{GL}_2(\mathbf{k}[x_3])$:

$$g = \begin{pmatrix} -x_3 & 1 \\ 1 & 0 \end{pmatrix}, \quad g^{-1} = \begin{pmatrix} 0 & 1 \\ 1 & x_3 \end{pmatrix}.$$

It is natural to define the following sequences in $\mathbf{k}[x_3]$:

$$\begin{aligned} &P_{-1} = 0, P_0 = 1, \text{ and for all } n \geqslant 1, P_n := x_3P_{n-1} + P_{n-2}, \\ &Q_{-1} = 0, Q_0 = 1, \text{ and for all } n \geqslant 1, Q_n := -x_3Q_{n-1} + Q_{n-2}. \end{aligned}$$

Then we have

$$g^n = \begin{pmatrix} Q_n & Q_{n-1} \\ Q_{n-1} & Q_{n-2} \end{pmatrix}, \quad g^{-n} = \begin{pmatrix} P_{n-2} & P_{n-1} \\ P_{n-1} & P_n \end{pmatrix}$$

and the stated properties follow by induction. □

LEMMA 7.11. – *Let $n \geqslant 2$ be even. For $m - l \geqslant 7$, there are only finitely many elements in* $\mathrm{Tame}(\mathbf{k}^3)$ *fixing the segment $\gamma[l,m]$.*

Proof. – Since f acts as a translation of length 2 on γ, it is sufficient to prove that there are only finitely many elements in $\mathrm{Tame}(\mathbf{k}^3)$ fixing the segment $\gamma[-2,4]$. So assume that $\phi^{-1} = (\phi_1, \phi_2, \phi_3)$ fixes $\gamma[-2,4]$. First, the fact that ϕ^{-1} fixes $\gamma(0) = [x_1]$ and $\gamma(2) = [x_3]$ means that

$$\phi_1 = ax_1 + b, \quad \phi_3 = cx_3 + d,$$

for some $a, c \in \mathbf{k}^*$, $b, d \in \mathbf{k}$. This implies that $\phi_2 = ex_2 + Q(x_1, x_3)$ for some $e \in \mathbf{k}^*$ and $Q \in \mathbf{k}[x_1, x_3]$. Now, using the notation from Lemma 7.10, we consider the action on

$$\gamma(4) = f \cdot [x_3] = [x_3 \circ h^{-1} \circ g^{-n}] = [x_2 \circ g^{-n}] = [x_1P_{n-1}(x_3) + x_2P_n(x_3)].$$

We have

$$\phi \cdot \gamma(4) = [(ax_1 + b)P_{n-1}(cx_3 + d) + (ex_2 + Q(x_1, x_3))P_n(cx_3 + d)],$$

and the condition $\phi \cdot \gamma(4) = \gamma(4)$ means that there exist α, β such that

$$(ax_1 + b)P_{n-1}(cx_3 + d) + (ex_2 + Q(x_1, x_3))P_n(cx_3 + d) \\ = \alpha x_1 P_{n-1}(x_3) + \alpha x_2 P_n(x_3) + \beta.$$

Since these polynomials are linear in x_2, we get in fact two equations

$$(ax_1 + b)P_{n-1}(cx_3 + d) + Q(x_1, x_3)P_n(cx_3 + d) = \alpha x_1 P_{n-1}(x_3) + \beta,$$
$$eP_n(cx_3 + d) = \alpha P_n(x_3).$$

Comparing the terms with factor x_3^n of the first equation gives $Q = 0$. By Lemma 7.10, P_n is even and hence on the right side of the second equation we have no x_3^{n-1} term, consequently $d = 0$. Thus our system of equations is now

$$(ax_1 + b)P_{n-1}(cx_3) = \alpha x_1 P_{n-1}(x_3) + \beta,$$
$$eP_n(cx_3) = \alpha P_n(x_3).$$

By Lemma 7.10 we have $P_n(0) = 1$ and $P_{n-1}(0) = 0$, so that we get successively

$$\alpha = e, \beta = 0, c = \pm 1, b = 0, \alpha = ca.$$

Finally, using the notation from Lemma 7.10, we have

$$\gamma(-2) = f^{-1} \cdot [x_1] = [x_1 \circ g^n \circ h] = [Q_n(x_1)x_2 + Q_{n-1}(x_1)x_3].$$

From the constraint $\phi \cdot \gamma(-2) = \gamma(-2)$, we have α', β' such that

$$Q_n(ax_1)ex_2 + Q_{n-1}(ax_1)cx_3 = \alpha' Q_n(x_1)x_2 + \alpha' Q_{n-1}(x_1)x_3 + \beta'.$$

Comparing the terms with factor x_2 we get

$$eQ_n(ax_1) = \alpha' Q_n(x_1).$$

Since $Q_n(0) = 1$ we get $e = \alpha'$, and then $a = \pm 1$. Summarizing, ϕ is in the diagonal group of order four $\{(ax_1, acx_2, cx_3); a = \pm 1, c = \pm 1\}$. □

Proof of Theorem D. – For any $C \geqslant 1$, let $2k \geqslant 24C + 6$. Let $x = \gamma(0)$. Suppose that we have $j \in \mathrm{Tame}(\mathbf{k}^3)$ with $v = j \cdot x$, $v' = j \circ f^k \cdot x$ at distance $\leqslant C$ from x, $f^k \cdot x = \gamma(2k)$, respectively. By Corollary 7.8, we have that $\alpha = j \cdot \gamma[0, 2k]$ is a geodesic from v to v'.

We will now prove that $\alpha \cap \gamma[0, 2k]$ has the form $\gamma[l, l']$. By Lemma 7.9, α intersects $\gamma[0, 2k]$. Let $l, l' \in [0, 2k]$ be minimal, and maximal, respectively, with $\gamma(l), \gamma(l') \in \alpha$. By Corollary 7.7, for any even $l \leqslant k' \leqslant l'$, the vertex $\gamma(k')$ lies in α. In fact, since any pair of type 1 vertices has at most one common neighbor of type 2, the entire $\gamma[l, l']$ lies in α.

Let m be such that $\gamma(l) = j \cdot \gamma(m)$. We first exclude the possibility that α and $\gamma[0, 2k]$ have reverse orientations on the common part, meaning $\gamma(l') = j \cdot \gamma(m - (l' - l))$. Indeed, then by Lemma 7.9 applied to $j \cdot \gamma[m + 1, 2k]$, we obtain $2k - l < 12C$. Analogously, we get $l' < 12C$ and consequently $2k < 24C$, which is a contradiction. Thus we have $\gamma(l') = j \cdot \gamma(m + (l' - l))$.

Hence the map $f^{(m-l)/2} \circ j$ fixes the entire $\gamma[m, m + (l' - l)]$. By Lemma 7.9 applied to $j \cdot \gamma[0, m - 1]$, we obtain $l < 12C$. Analogously, $2k - l' < 12C$. Consequently, $l' - l > 2k - 12C - 12C = 2k - 24C \geqslant 6$. By Lemma 7.11, there are only finitely many such j. This shows that f is WPD. □

REMARK 7.12. – The complex $\mathcal{C}$ does not satisfy an isoperimetric inequality in the following sense. Consider an infinite geodesic path in $\mathscr{T}([x_1, x_2])$ starting at $v^0 = [x_1]$ and passing successively through vertices $v^1, v^2, \ldots$ of type 1. Let α_n be the length 8 loop in $\mathcal{C}$ passing through type 1 vertices $v^0, [x_3], v^n, [x_3 + x_1^2]$. Since the two neighbors of $[x_3]$ on α_n are at distance $2n$ in $\mathscr{L}([x_3])$, the minimal area of disk diagrams bounded by α_n converges to ∞.

Thus for WPD we cannot apply [16, Lem 2.11] of A. Martin to prove that $\mathcal{C}$ has Strong Concatenation Property. In fact, the first condition of his Strong Concatenation Property fails if we split α_n into paths γ_1, γ_2 from $[x_3]$ to $[x_3 + x_1^2]$ yielding $A \geqslant 2n$.

However, one can recognize variants of the two conditions of his Thm 1.2 guaranteeing WPD in our Lemmas 7.9 and 7.11. In Lemma 7.11 we prove a slightly weaker result than the one needed to apply his Thm 1.2 directly, but in the proof of Theorem D we actually establish his condition using Corollary 7.8.

BIBLIOGRAPHY

[1] M. BESTVINA, K. FUJIWARA, Bounded cohomology of subgroups of mapping class groups, *Geom. Topol.* **6** (2002), 69–89.

[2] C. BISI, J.-P. FURTER, S. LAMY, The tame automorphism group of an affine quadric threefold acting on a square complex, *J. Éc. polytech. Math.* **1** (2014), 161–223.

[3] B. H. BOWDITCH, Tight geodesics in the curve complex, *Invent. math.* **171** (2008), 281–300.

[4] M. R. BRIDSON, A. HAEFLIGER, *Metric spaces of non-positive curvature*, Grundl. math. Wiss. **319**, Springer, 1999.

[5] S. CANTAT, Sur les groupes de transformations birationnelles des surfaces, *Ann. of Math.* **174** (2011), 299–340.

[6] S. CANTAT, The Cremona group in two variables, in *European Congress of Mathematics*, Eur. Math. Soc., 2013, 211–225.

[7] S. CANTAT, S. LAMY, Normal subgroups in the Cremona group, *Acta Math.* **210** (2013), 31–94.

[8] F. DAHMANI, V. GUIRARDEL, D. OSIN, Hyperbolically embedded subgroups and rotating families in groups acting on hyperbolic spaces, *Mem. Amer. Math. Soc.* **245** (2017).

[9] V. I. DANILOV, Non-simplicity of the group of unimodular automorphisms of an affine plane, *Mat. Zametki* **15** (1974), 289–293.

[10] J.-P. FURTER, S. LAMY, Normal subgroup generated by a plane polynomial automorphism, *Transform. Groups* **15** (2010), 577–610.

[11] T. JANUSZKIEWICZ, J. ŚWIĄTKOWSKI, Simplicial nonpositive curvature, *Publ. Math. Inst. Hautes Études Sci.* **104**, 1–85.

[12] S. KURODA, Shestakov-Umirbaev reductions and Nagata's conjecture on a polynomial automorphism, *Tohoku Math. J.* **62** (2010), 75–115.

[13] S. LAMY, Combinatorics of the tame automorphism group, arXiv:1505.0549, to appear in *Ann. Fac. Sci. Toulouse*.

[14] A. Lonjou, Non simplicité du groupe de Cremona sur tout corps, *Ann. Inst. Fourier* **66** (2016), 2021–2046.

[15] R. C. Lyndon, P. E. Schupp, *Combinatorial group theory*, Ergebn. Math. Grenzg. **89**, Springer, 1977.

[16] A. Martin, On the acylindrical hyperbolicity of the tame automorphism group of $\mathrm{SL}_2(\mathbf{C})$, *Bull. London Math. Soc.* **49** (2017), 881–894.

[17] A. Minasyan, D. Osin, Acylindrical hyperbolicity of groups acting on trees, *Math. Ann.* **362** (2015), 1055–1105.

[18] D. Osin, Acylindrically hyperbolic groups, *Trans. Amer. Math. Soc.* **368** (2016), 851–888.

[19] J-P. Serre, *Trees*, Springer, 1980.

[20] I. P. Shestakov, U. U. Umirbaev, The tame and the wild automorphisms of polynomial rings in three variables, *J. Amer. Math. Soc.* **17** (2004), 197–227.

[21] D. Wright, The generalized amalgamated product structure of the tame automorphism group in dimension three, *Transform. Groups* **20** (2015), 291–304.

(Manuscrit reçu le 18 octobre 2016 ;
accepté, après révision, le 19 septembre 2017.)

Stéphane Lamy
Institut de Mathématiques de Toulouse, UMR 5219
Université de Toulouse, UPS
31062 Toulouse Cedex 9, France
E-mail: slamy@math.univ-toulouse.fr

Piotr Przytycki
Dept. of Math. & Stats.
McGill University
Montréal, Québec, Canada H3A 0B9
E-mail: piotr.przytycki@mcgill.ca